HHS Public Access

Author manuscript

New Phytol. Author manuscript; available in PMC 2023 August 01.

Published in final edited form as:

New Phytol. 2022 August ; 235(3): 1057–1069. doi:10.1111/nph.18156.

ABA negatively regulates the Polycomb-mediated H3K27me3 through the PHD-finger protein, VIL1

Wei Zong[1,*], **Junghyun Kim**[1,*], **Yogendra Bordiya**[1], **Hong Qiao**[1], **Sibum Sung**[1]

[1]Department of Molecular Biosciences, The University of Texas at Austin, Austin, TX 78712, USA

Summary

- Polycomb dictates developmental programs in higher eukaryotes, including flowering plants. A phytohormone, Abscisic acid (ABA), plays a pivotal role in seed and seedling development and mediates responses to multiple environmental stresses, such as salinity and drought.
- In this study, we show that ABA affects the Polycomb Repressive Complex 2 (PRC2)-mediated Histone H3 Lys 27 trimethylation (H3K27me3) through VIN3-LIKE1/VERNALIZATION 5 (VIL1/VRN5) to fine-tune the timely repression of *ABSCISIC ACID INSENSITIVE 3* (*ABI3*) and *ABSCISIC ACID INSENSITIVE 4* (*ABI4*) in *Arabidopsis thaliana*.
- *vil1* mutants exhibit hypersensitivity to ABA during early seed germination and show enhanced drought tolerance.
- Our study revealed that the ABA signaling pathway utilizes a facultative component of the chromatin remodeling complex to demarcate the level of expression of ABA-responsive genes.

Keywords

Arabidopsis; ABA; germination; drought tolerance; VIL1; PRC2

Correspondence: sbsung@austin.utexas.edu.

*These authors equally contribute to the manuscript.

Author Contributions

W. Z., J. K., Y. B., H. Q., and S. S. conceived of and implemented the method, performed the experiments and data analysis. W. Z., J. K. and S. S. drafted the manuscript. S. S. advised on the design and implementation, and interpretation of results and edited the manuscript. All authors read and approved the final manuscript.

Supplementary Information

Table S1. Primers used in this study.

Table S2. Differentially expressed gene in *vil1*.

Fig. S1 Differentially expressed genes in *vil1* mutants.

Fig. S2 VIL1 regulates ABA response in *Arabidopsis*.

Fig. S3 VIL1 represses *ABI3* and *ABI4* expression during germination.

Fig. S4 The H3K27me3 levels at *ABI5* locus during seed germination.

Fig. S5 VIL1 expressions are not regulated by ABA treatment.

Fig. S6 CLF and SWN directly bind to *ABI3* and *ABI4* but not to *ABI5*.

Fig. S7 VIL1 functions together with PRC2 components to regulate the ABA response.

Fig. S8 Seed phenotype of Col-0, *vil1*, *abi3,* and *vil1 abi3* double mutants in *Arabidopsis*.

Fig. S9 Water loss assay in *Arabidopsis*.

Fig. S10 Working model showing that VIL1-PRC2 regulates seed germination in *Arabidopsis*.

Introduction

Abscisic acid (ABA) is a phytohormone that plays essential roles in seed dormancy, seed germination, seedling growth, stomata closure, water usage, and stress responses (Cutler *et al.*, 2010; Chen, K *et al.*, 2020; Zhang *et al.*, 2020). ABA accumulates in the developing embryo but declines rapidly upon imbibition, which precedes seed germination and early seedling growth (Gubler *et al.*, 2005; Weitbrecht *et al.*, 2011). Exogenous ABA treatment inhibits seed germination and early seedling growth, and several ABA-insensitive (*ABI*) genes have been identified based on the lack of response to the ABA treatment (Finkelstein *et al.*, 2002). Among *ABI* genes, *ABI3*, *ABI4*, and *ABI5* encode transcription factors containing B3, APETALA2-like, and basic leucine zipper (bZIP) domains for DNA bindings, respectively (Giraudat *et al.*, 1992; Finkelstein *et al.*, 1998; Finkelstein & Lynch, 2000). *ABI1* and *ABI2* are involved in ABA signaling and encode protein phosphatase 2Cs (PP2Cs) (Cutler *et al.*, 2010; Chen, K *et al.*, 2020). PYR/PYL/RCAR family of ABA receptors antagonize PP2Cs, including ABI1 and ABI2, upon the ABA binding, and this, in turn, results in the accumulation of phosphorylated forms of SNF1-related protein kinases (SnRK2s) (Fujii *et al.*, 2009; Ma *et al.*, 2009; Park *et al.*, 2009). Activated SnRK2s phosphorylate several transcription factors to trigger a cascade of transcriptional regulation (Cutler *et al.*, 2010; Chen, K *et al.*, 2020). For example, RAV (Related to ABI3/VP1)-class transcription factor RAV1 is phosphorylated by SnRK2s and regulates expressions of early ABA-responsive transcription factors, including *ABI3*, *ABI4*, and *ABI5* (Feng *et al.*, 2014). *ABI3*, *ABI4*, and *ABI5* transcripts accumulate in developing embryos but rapidly decrease upon germination and during early seedling development, indicating that dynamic transcriptional regulatory network functions to control the expression of *ABI3*, *ABI4*, and *ABI5* during seed and early seedling development (Jia *et al.*, 2014; Chandrasekaran *et al.*, 2020). In addition, these transcription factors are induced upon the ABA treatment by triggering the ABA signaling pathway to mediate downstream transcriptional cascades (Jia *et al.*, 2014; Chandrasekaran *et al.*, 2020).

Polycomb Repressive Complex 2 (PRC2) is an evolutionarily conserved chromatin-modifying enzyme complex that mediates Histone H3 Lys 27 trimethylation (H3K27me3) at developmentally controlled loci in eukaryotes (Mozgova & Hennig, 2015; Yu *et al.*, 2019). PRC2 consists of four core subunits, including Enhancer of Zeste (E(z)), Extra Sex Combs (ESC), WD40-containing protein (Nurf55), and Suppressor of Zeste 12 (Su(z)12) in a stoichiometric ratio of 1:1:1:1 (Ciferri *et al.*, 2012). In *Arabidopsis*, multiple genes encode four core subunits with some functional redundancies (Mozgova & Hennig, 2015). Three homologous genes for the E(z) methyltransferases are *MEDEA* (*MEA*), *CURLY LEAF* (*CLF*), and *SWINGER* (*SWN*), and a single homologous gene for *ESC* is *FERTILIZATION INDEPENDENT ENDOSPERM* (*FIE*) (Mozgova & Hennig, 2015). Five *Nurf55*-like genes, *MULTICOPY SUPPRESSOR OF IRA1-5* (*MSI1-5*), and three *Su(z)12*-like genes, *FERTILIZATION INDEPENDENT SEED 2* (*FIS2*), *EMBRYONIC FLOWER2* (*EMF2*), and *VERNALIZATION2* (*VRN2*), exist in the *Arabidopsis* genome (Mozgova & Hennig, 2015). Three distinct PRC2 complexes function in various aspects of developmental transitions in *Arabidopsis*. The FIS2 complex uses MEA as a sole E(z) methyltransferase and includes FIS2, FIE, and MSI1 (Baroux *et al.*, 2006; Hennig & Derkacheva, 2009).

The FIS2 complex functions only in the female gametophyte and endosperm but not in the sporophyte (Hennig & Derkacheva, 2009). In sporophyte, two PRC2 complexes, the EMF2 complex (EMF2, FIE, CLF or SWN, and MSIs) and the VRN2 complex (VRN2, FIE, CLF or SWN, and MSIs), function by utilizing two E(z) homologs, CLF and SWN, redundantly (Chanvivattana *et al.*, 2004; De Lucia *et al.*, 2008; Hennig & Derkacheva, 2009; Mozgova & Hennig, 2015). *clf swn* double mutants exhibit multiple developmental defects including developmental arrest at seedling stage, illustrating the pivotal function of PRC2 complexes in plant development (Chanvivattana *et al.*, 2004; Farrona *et al.*, 2011; Shu *et al.*, 2019). The EMF2 complex is involved in developmental transitions, and the VRN2 complex is known to repress *FLOWERING LOCUS C* (*FLC*) in response to winter cold (Gendall *et al.*, 2001; De Lucia *et al.*, 2008; Kim *et al.*, 2012). In mammals and *Drosophila*, the core of PRC2 is also associated with a number of facultative subunits which facilitate the PRC2 activity, providing a regulatory flexibility in regulating gene expression (Mozgova & Hennig, 2015; Yu *et al.*, 2019). Similarly, genetic and biochemical studies revealed that the VRN2 complex is associated with the PHD-finger containing the VERNALIZATION INSENSITIVE 3 (VIN3) family proteins, including VIN3, VIN3-LIKE 1 (VIL1), and VIL2 (De Lucia *et al.*, 2008). The VIN3 family proteins are necessary for the repression of *FLC* by the VRN2 complex (De Lucia *et al.*, 2008; Kim & Sung, 2013).

Although PRC2 plays roles in many aspects of plant development, its involvement in seed germination has not been studied. Seed germination is controlled in part by ABA signaling pathway that determined the balance between seed dormancy and germination (Jia *et al.*, 2014). The ABA signaling pathway eventually elicits the cascade of transcriptional regulations, and several key transcription factors have been identified (Chen, K *et al.*, 2020; Zhang *et al.*, 2020). Although the prominent roles of the DNA-binding transcription factors in ABA signaling pathway have been extensively studied (Chen, K *et al.*, 2020), chromatin-modifying complexes are also expected to be involved in transcriptional regulation of the ABA signaling pathway (Peirats-Llobet *et al.*, 2016; Bulgakov *et al.*, 2019; Lee & Seo, 2019; Liu *et al.*, 2019). However, defects in many chromatin-remodeling complexes also compromise multiple developmental processes which make it difficult to address biological significance of the roles of chromatin-remodeling complexes in the ABA signaling. Here, we report that the *vil1* mutant is hypersensitive to the ABA treatment and exhibits enhanced drought tolerance. Our study shows that VIL1-PRC2 is necessary to properly repress ABA-signaling transcription factors, including *ABI3* and *ABI4*. We identified the molecular regulatory mechanism by which VIL1 limits the induction of ABA-responsive genes to coordinately regulate ABA-mediated transcriptional changes that lead to proper early seedling development and drought response.

Materials and Methods

Plant materials and growth conditions

Arabidopsis thaliana (L.) accession Columbia (Col-0), *vil1* (SALK_136506), *vil1-2* (SALK_140132), *clf* (SALK_106381), *swn* (SALK_050195), *abi3* (SALK_138922), *abi4* (CS8104) and *abi5* (SALK_013163) lines were obtained from Arabidopsis Biological Resource Center (Columbus, OH). To generate complement lines p*VIL1*:*VIL1-myc*/*vil1* and

p*VIL1*:*VIL1-flag*/*vil1*, the *VIL1* genomic DNA was first cloned into the pENTR_dTOPO vector and further transferred to pGWB16 or pEarleyGate 302 vectors, respectively. *vil1 abi3_cri* was generated by CRISPR/Cas9 method (Xing *et al.*, 2014; Wang *et al.*, 2015; Liu *et al.*, 2017). The constructs above were transformed into Agrobacterium tumefaciens cells (GV3101) and then stably transformed into *Arabidopsis* using the floral dip method (Clough & Bent, 1998). The complementation lines of p*CLF*:*CLF-GFP*/*clf29* (*gCLF-GFP*) and p*SWN*:*SWN-GFP*/*swn-4* (*gSWN-GFP*) were previously described (Shu *et al.*, 2019). Higher-order mutants were generated by genetic crossing. Plants were grown in controlled environmental chambers with cool white fluorescent lights and maintained at 22°C. The photoperiodic cycle was 16 h light/8 h dark (long day, LD) and 8 h light/16 h dark (short day, SD).

ABA treatment

Seeds collected at the same time were used for ABA treatment assays. For germination assays, surface-sterilized seeds were plated on half-strength Murashige & Skoog medium (½MS medium) supplemented with or without the indicated concentration of ABA and then stratified at 4°C in darkness for 3 days. The germination rates (green cotyledon) were counted at the indicated time points. For root growth assays, seeds were germinated on ½MS medium for 3 days, followed by transfer to ½MS medium with or without 10 μM ABA. Plates were incubated vertically for an additional 7 days before measuring primary root length by Image J. For long-term ABA treatment for gene expression and ChIP analysis, seeds were spread on a filter paper, which plated on ½MS medium supplemented with or without 0.5 μM ABA and then stratified at 4°C in darkness for 3 days followed by growth in long-day growth chambers for another 3 days. For short-term ABA treatment for gene expression and ChIP analysis, seeds were spread on a filter paper, which plated on ½MS medium and then stratified at 4°C in darkness for 3 days followed by growth in long-day growth chambers for another 3 days. Filter papers with germinated seedlings were moved into liquid ½ MS medium with or without 50 μM ABA for 4 h.

Drought stress and dehydration treatment

For the drought tolerance analysis, 5-day-old seedlings grown on ½ MS medium were transferred to thoroughly watered soil: turface (3:1) and grown in 12h light /12 dark condition. To avoid positional bias, different genotypes were grown at various sites of the pot. After 20 days of growth without water, watering was resumed, and phenotypes were recorded 3 days after watering. For dehydration treatment, 7-day-old seedlings grown on ½ MS medium were exposed to the air by removing the petri dish lid. After 5 days, seedlings were rehydrated. Survival rates were counted, and pictures were taken 1 day after rehydration. Seedlings that have more than two green leaves were counted as surviving.

Water loss Experiments

For water loss rate measurement, rosette leaves were detached from 3-week-old plants grown in long-day condition or 5-week-old plants grown in short-day condition, weighed immediately on weighting paper, and then placed on the laboratory bench. The weight losses of the samples were measured at designated time points (as indicated in Fig. 7). The proportion of water loss rate was calculated based on the initial fresh weight of the samples.

mRNA expression analysis

Total RNA was prepared using PureLink™ Plant RNA Reagent (Invitrogen). For reverse-transcription followed by quantitative PCR (RT-qPCR), 1 μg total RNAs were treated with DNase I (Invitrogen) before reverse transcription, and then the first-strand cDNA was synthesized by M-MLV (Invitrogen). RT-qPCR was performed using ViiA 7 Real-Time PCR System (Applied Biosystems) and AzuraQuant™ Green Fast qPCR Mix (Azura Genomics). Arabidopsis constitutively expressed *PP2A* (AT1g69960) was used as an internal control for normalization. The primers used for RT-qPCR are listed in Table S1.

Protein Extraction and western blot

For protein extraction, seedlings were frozen in liquid nitrogen and homogenized with urea-denaturing buffer (100 mM NaH_2PO_4, 10 mM Tris-HCl (pH 8.0), 8M Urea, 1 mM PMSF, Protease inhibitor cocktails). The debris was removed by centrifugation at 12,000 g at 4°C for 10 min. Extracted proteins were denatured by boiling at 100°C for 10 min with 1X SDS sample buffer. Western blot was performed to check VIL1-myc protein levels using anti-myc antibody (Santa Cruz, c-myc (9E10) X antibody, sc-40X, 1:5,000 dilution). Tubulin levels were detected by anti-α-Tubulin antibody (T5168, 1:10,000 dilution). Ponceau S staining was performed to minimize any discrepancies in protein amount.

RNA-Seq analysis

The total RNA was extracted from 1-day-old seedlings using PureLink™ Plant RNA Reagent (Invitrogen). For each sample, three independent replicates were used. Genomic Sequencing and Analysis Facility, the University of Texas at Austin, performed the library preparation and sequencing. Briefly, a total amount of 1 μg RNA per sample was used for 3'-TagSeq library preparations. Prepared libraries were sequenced by NovaSeq 6000 System (Illumina). The reads were mapped to the TAIR 10 Arabidopsis genome using Bowtie 2. Differentially expressed genes were identified by using DESeq 2 with default parameters. Genes with at least a 1.5-fold change in expression and $P < 0.05$ between mutant and WT (Col-0) were considered differentially expressed genes (DEGs). The gene ontology of DEGs in *vil1* mutant was performed by the AgriGO v2.0 with default parameters (Tian *et al.*, 2017). The Heat map to show the enriched gene ontology categories was performed by TBtools (Chen, C *et al.*, 2020).

Chromatin immunoprecipitation (ChIP)

ChIP experiments were performed as previously reported (Zong *et al.*, 2021). Briefly, 1 g seedlings were used for nuclei isolation. Chromatin was sheared by using a Bioruptor® to an average size of about 500 bp. Sheared chromatin was further diluted in ChIP dilution buffer and incubated with 4 μg (Santa Cruz, c-myc (9E10) X antibody, sc-40X), H3K27me3 (07–449; Millipore Sigma) or GFP (ab290; Abcam) antibodies overnight at 4°C. Antibody was further captured by Dynabeads Protein G (Thermo Fisher Scientific) and then washed by low salt, high salt, LiCl, and TE buffers. The DNA-protein complex was eluted, and reverse cross-linked at 65°C overnight. DNA was purified by using QIAquick® PCR Purification Kit (Qiagen) and was used for qPCR analysis (Primers listed in Table S1).

Statistical analysis

Two-tailed Student's t-test and One-way ANOVA followed by Tukey HSD test for multiple comparisons were conducted using Prism 8.

Results

VIL1 negatively regulates the ABA response

Although VIL1 is best known as a component of PRC2 that mediates H3K27me3 at the *FLC* locus upon vernalization (Sung *et al.*, 2006; Greb *et al.*, 2007; De Lucia *et al.*, 2008), VIL1 also appears to function in other developmental processes, including photoperiodic flowering (Sung *et al.*, 2006) and light signaling (Kim *et al.*, 2021). To elucidate the roles of VIL1 in early developmental processes, we performed transcriptome analysis using 1-day-old seedlings of wild type and *vil1* mutants (Fig. S1a; Table S1). Gene ontology (GO) analysis of differentially expressed genes (DEGs) in *vil1* mutants showed that GO terms of stress responses, hormone signaling, and seed germination processes are significantly enriched in up-regulated DEGs but not in down-regulated DEGs in *vil1* mutants (Fig. S1b). Interestingly, terms related to "in response to abscisic acid (ABA)" are among significant up-regulated DEGs in *vil1* mutants. VIL1 is a transcriptional repressor as a component of PRC2 (Sung *et al.*, 2006; Greb *et al.*, 2007; De Lucia *et al.*, 2008). Therefore, de-repression of ABA-related genes in *vil1* mutants implies that VIL1 plays role in ABA-related responses through gene repression.

To investigate whether VIL1 is involved in the ABA responses, we first examined the germination response in *vil1* mutants. Interestingly, the germination rate of the *vil1* mutants was significantly decreased after the ABA treatment when compared to the wild-type (WT, Col-0) and the complemented line (*gVIL1*) (Fig. 1a,b). The ABA hypersensitive phenotype of *vil1* mutants was further confirmed by using another allele (*vil1-2*) and an additional complemented line (*gVIL1-FLAG*) (Fig. S2). Moreover, the growth of the primary root of *vil1* mutants was also inhibited by the ABA treatment to a greater extent than WT root (Fig. 1c,d). Thus, these results indicate that VIL1 negatively regulates the ABA signaling in *Arabidopsis*.

VIL1 directly represses *ABI3* and *ABI4*

To understand how VIL1 regulates the ABA responses in *Arabidopsis*, we further investigated the gene expression profiles in *vil1* mutants. A total of 919 DEGs were identified in 1-day-old seedlings of *vil1* mutants (Fig. S1a; Table S2). Three ABA signaling transcription factors, *ABI3*, *ABI4*, and *ABI5*, were among the up-regulated DEGs in *vil1* mutants. These three transcription factors are rather quickly repressed during early seed germination process and constitute a crucial transcription regulatory hub in ABA signaling (Lopez-Molina *et al.*, 2001; Perruc *et al.*, 2007; Chandrasekaran *et al.*, 2020). To test whether VIL1 was required for the repression of *ABI3*, *ABI4,* and *ABI5* during the seed germination, we first investigated the expression levels of *ABI3*, *ABI4,* and *ABI5* in the *vil1* mutant at different germination stages. Interestingly, we found that *ABI3*, *ABI4,* and *ABI5* are increased in the *vil1* mutant only during the early germination stages (1 to 5 days after germination (DAG)), but not in dry seeds or at later germination stage (7 DAG) (Fig. S3),

suggesting that *VIL1* is necessary for establishing the repression of these transcription factor genes during early stages of germination.

ABA treatment increases the expression of *ABI3*, *ABI4,* and *ABI5* in WT (Perruc *et al.*, 2007; Chandrasekaran *et al.*, 2020). Interestingly, the expression levels of *ABI3*, *ABI4,* and *ABI5* are even higher in *vil1* mutants compared to WT (Fig. 2a), indicating that VIL1 limits the induction of *ABI3*, *ABI4,* and *ABI5* upon the ABA treatment. To explore whether VIL1 directly binds to *ABI3, ABI4,* and *ABI5* genomic regions, we employed chromatin immunoprecipitation followed by quantitative PCR (ChIP-qPCR) assays. Indeed, we observed the enrichment of VIL1 at *ABI3* and *ABI4* genomic regions, but not at *ABI5* locus, at 3 DAG (Fig. 2b–d). Interestingly, the levels of VIL1 enrichment at *ABI3* and *ABI4* loci significantly decreased at the gene body regions of *ABI3* and *ABI4* when treated with ABA (Fig. 2b–d), indicating that the removal of VIL1 from *ABI3* and *ABI4* chromatin occurs in response to ABA treatment, concurrent with the de-repression of *ABI3* and *ABI4*.

VIL1 is necessary for the H3K27me3-mediated repression of *ABI3* and *ABI4*

Because VIL1 is known to promote PRC2 function, the H3K27 methylation, we also measured the level of H3K27me3 at *ABI3*, *ABI4*, and *ABI5* loci (Fig. 3a,b). Consistent with the direct association of VIL1 with *ABI3* and *ABI4* chromatin, the levels of H3K27me3 are significantly lower at *ABI3* and *ABI4* loci in *vil1* mutants (Fig. 3a,b). Furthermore, ABA treatment reduces the level of H3K27me3 at *ABI3* and *ABI4* loci (Fig. 3a,b), indicating that the reduction in VIL1 enrichment by ABA results in the decrease in the levels of H3K27me3 at *ABI3* and *ABI4*. On the other hand, no significant H3K27me3 enrichment was observed at the *ABI5* locus regardless of the ABA treatment (Fig. 3b), indicating that *ABI5* is not under the control of VIL1-mediated H3K27me3 (Fig. 2d, 3b).

Transcriptional repression is triggered at *ABI3*, *ABI4*, and *ABI5* loci during early germination (Lopez-Molina *et al.*, 2001; Perruc *et al.*, 2007; Chandrasekaran *et al.*, 2020). We observed that the levels of H3K27me3 increase rapidly during early germination at *ABI3* and *ABI4* chromatin but not at *ABI5* chromatin (Fig. 3c,d, Fig. S4). Furthermore, the increases in the level of H3K27me3 at *ABI3* and *ABI4* are compromised in *vil1* mutants (Fig. 3c,d). It is known that the repression of *ABI3* and *ABI4* after germination is achieved by the various combinations of their transcriptional activators and repressors (Parcy *et al.*, 1997; To *et al.*, 2006; Feng *et al.*, 2014). The reduced levels of H3K27me3 at *ABI3* and *ABI4* in *vil1* mutants correlate with the de-repression of *ABI3* and *ABI4* at the early stages of germination, but both *ABI3* and *ABI4* are eventually repressed both in WT and *vil1* mutants at later stage of gemination (Fig. S3), indicating that the VIL1-mediated H3K27me3 is necessary for the rapid repression of *ABI3* and *ABI4* at the early stage of germination. Taken together, our results show that VIL1 directly associates with *ABI3* and *ABI4* chromatin to repress their expressions by modulating H3K27me3 levels during early seed germination.

ABA-responsive activation of *ABI3* and *ABI4* includes the removal of VIL1 to reduce H3K27me3

We observed that the ABA-triggered induction of *ABI3* and *ABI4* accompanies the reduced enrichment of VIL1 and H3K27me3 at *ABI3* and *ABI4* loci (Fig. 2c,d, Fig. 3a,b). Significant induction of *ABI3* and *ABI4* transcripts is observed with 4 hours of ABA treatment (Fig. 4a–c). Interestingly, reductions in the enrichment of VIL1 at these loci also occur rapidly as short as 4 hours of the ABA treatment (Fig. 4d). Consistent with the rapid reduction in the enrichment of VIL1, the levels of H3K27me3 at both *ABI3* and *ABI4* decrease by the 4-hour ABA treatment (Fig. 4e). However, the expression of *VIL1* is not affected by the ABA treatment both in the levels of mRNA and protein (Fig. S5). Therefore, ABA affects the VIL1 enrichment at *ABI3* and *ABI4* loci.

Given that VIL1 is a facultative component of PRC2 (De Lucia *et al.*, 2008; Derkacheva *et al.*, 2013; Wang *et al.*, 2016), we first investigated whether *ABI3* and *ABI4* are direct targets of the core components of PRC2. Indeed, a genome-wide occupancy study of CLF and SWN in *Arabidopsis* indicates that both CLF and SWN bind to *ABI3* and *ABI4* loci, but not to *ABI5* locus (Fig. S6a), which is consistent with the occupancy patterns of VIL1 (Fig. 2c,d). We also confirmed that CLF and SWN are enriched at *ABI3* and *ABI4* loci, but not at *ABI5* locus by ChIP-qPCR (Fig. S6b,c). In addition, H3K27me3 is not detectable at *ABI3* and *ABI4* in *clf swn* double mutants (Shu *et al.*, 2019), indicating that CLF and SWN redundantly control the deposition of H3K27me3 at these loci. On the other hand, *ABI5* chromatin is not enriched with H3K27me3, consistent with that *ABI5* is not enriched with CLF, SWN, and VIL1 (Fig. 2d, S6a).

Because the VIL1 enrichment at the *ABI3* and *ABI4* locus is rapidly reduced by ABA treatment (Fig. 4d), we tested whether the core components of PRC2 are also rapidly removed from the *ABI3* and *ABI4* loci upon the ABA treatment (Fig. 4h). We measured changes in enrichments of two E(z) homologs, CLF and SWN at *ABI3* and *ABI4* loci upon ABA treatment by ChIP-qPCR. Although CLF and SWN occupy both *ABI3* and *ABI4* chromatin (Fig. S6a–c), the enrichment of CLF and SWN at *ABI3*, but not at *ABI4*, slightly decreases under long-term ABA treatment, and not affected at all by the short-term ABA treatment (Fig. 4f,g). Therefore, the enrichment of VIL1 at *ABI3* and *ABI4* is critical for the PRC2 activity and its rapid removal by ABA is a part of regulatory modules in the ABA-mediated transcriptional response. Taken together, our data collectively show that the dynamic nature of VIL1-mediated H3K27me3 contributes to the regulation of ABA-responsive genes.

VIL1 mediates the PRC2 activity to specifically regulate the ABA responses

We attempted to address the roles of CLF and SWN in VIL1-mediated ABA responses by examining the ABA responses of the corresponding mutants (Fig. S7). Unlike the *vil1* mutant, which is hypersensitive to ABA, neither *clf* nor *swn* single mutant shows strong ABA hypersensitivity as determined by cotyledon greening (Fig. S7). The *clf* single mutant is slightly hyposensitive to the ABA treatment, and the *vil1 clf* double mutant also shows a higher cotyledon-greening rate than the *vil1* single mutant (Fig. S7a,b). On the other hand, the *swn* single mutant exhibits a slight ABA hypersensitive phenotype similar to the *vil1*

mutant, and the *vil1 swn* double mutant shows a synergistically enhanced ABA sensitivity (Fig. S7c,d). The *clf swn* double mutant exhibits aberrant early seedling development (Shu *et al.*, 2019), and therefore we could not address the ABA responses in *clf swn* double mutants. In *clf* mutants, both *ABI3* and *ABI4* are slightly lower than WT at 3 DAG, while the expressions of *ABI3* and *ABI4* are not significantly changed in *swn* mutants (Fig. 5a,b). Neither *clf* nor *swn* single mutants significantly de-repress the expression of *ABI3* and *ABI4* to the comparable level observed in the *vil1* mutant (Fig. 5a,b), indicating that CLF and SWN redundantly function together with VIL1 to de-repress *ABI3* and *ABI4* during early seed germination. We also found the H3K27me3 levels at *ABI3* and *ABI4* chromatin were largely correlated with the expression levels of *ABI3* and *ABI4* (Fig. 5c,d). Interestingly, the level of *ABI3* expression is lower in *clf* mutants at 3 DAG, consistent with the slightly higher level of H3K27me3 at *ABI3* in *clf* mutants (Fig. 5a). This observation may indicate possible over-compensation by SWN in *clf* mutants or other ABA-signaling factors under the control of CLF. Our results indicate that VIL1 promotes the function of both CLF and SWN during seed germination to properly repress *ABI3* and *ABI4* in the absence of ABA.

VIL1 regulates ABA signaling through *ABI3* and *ABI4*

Our data show that VIL1 is directly associated with *ABI3* and *ABI4* to repress their expressions during early germination (Fig. 2). VIL1/PRC2-mediated H3K27me3 appears not to control the expression of *ABI5* directly. The differential expression of *ABI5* observed in *vil1* mutants is likely because ABI5 acts downstream of ABI3 and ABI4 (Lopez-Molina *et al.*, 2002; Bossi *et al.*, 2009). To genetically determine whether the increased levels of *ABI3*, *ABI4,* and *ABI5* caused the ABA hypersensitive phenotype of *vil1* mutants, we examined the ABA response of *vil1 abi5* and *vil1 abi4* double mutants. *vil1 abi5* double mutants restore the ABA insensitive phenotype of *abi5* single mutant, but *vil1 abi5* double mutants rather slowly restored the ABA insensitive phenotype of *abi5* at the later stage of germination (Fig. 6a). The ABA hypersensitive effect by the *vil1* mutant reverses in *vil1 abi4* double mutants and the double mutants show no difference compared to *abi4* single mutants after 3 DAG (Fig. 6b), although the ABA insensitive phenotype of *abi4* was partially restored in *vil1 abi4* double mutants at the early stage of germination (Fig. 6b).

As *VIL1* and *ABI3* are located very close to each other in the *Arabidopsis* genome, we could not isolate the *vil1 abi3* double mutant by genetic crossings. Therefore, we mutated *ABI3* by CRISPR/Cas9 method (Liu *et al.*, 2017) in *vil1* mutant background to create *vil1 abi3_c* double mutants (Fig. S8a,b). Consistent with previously reported *abi3* deletion mutant alleles (Nambara *et al.*, 1994), all confirmed CRISPR/Cas9-generated mutants produce green seeds that are intolerant to desiccation (Fig. S8c). To validate the genetic relationship between *VIL1* and *ABI3*, three independent CRISPR/Cas9 lines of *vil1 abi3_c* double mutants (#41, #51, and #89) were selected and compared their responses to the ABA treatment with *abi3* and *vil1* single mutants (Fig. 6c, S8c). Interestingly, the germination rate of *vil1 abi3_c* double mutants show no difference compared to *abi3* single mutant even at higher ABA concentrations (Fig. 6c), suggesting that *abi3* is completely epistatic to *vil1*. Therefore, our genetic analysis, combined with the de-repression of *ABI3* and *ABI4* observed in *vil1* mutants, supports that VIL1 promotes seed germination through the deposition of H3K27me3 at *ABI3* and *ABI4* chromatin to repress their expressions.

vil1 mutants exhibit enhanced drought tolerance

Given that the *vil1* mutant is hypersensitive to ABA treatment at the early germination stage, we also addressed whether VIL1 may be involved in other stress responses. ABA is a key phytohormone in controlling water usage in plants (Cutler *et al.*, 2010; Chen, K *et al.*, 2020; Zhang *et al.*, 2020). Therefore, we examined the effect of *vil1* mutations on drought response. Surprisingly, *vil1* mutants had an increased survival rate under drought stress than WT (Fig. 7a). The drought tolerance phenotype observed in *vil1* mutants is consistent with the ABA hypersensitivity observed during seed germination in *vil1* mutants. Consistent with the drought tolerance observed in *vil1* mutants, water loss assays using detached leaves also showed that *vil1* mutants have much lower water-loss rates than WT and the complementation line (*gVIL1*) (Fig. 7b, S9a). Similar results were observed in dehydration stress assays, where mutations in *VIL1* resulted in an improved tolerance to dehydration stress (Fig. S9b,c).

Dehydration condition triggers the induction of several stress-related genes, including the dehydration-responsive gene, *RD29A* (Nakashima *et al.*, 2006). We also identified *RD29A* among DEGs in *vil1* mutants (Table S2). Indeed, *RD29A* is induced at a much higher level in *vil1* mutant background under dehydration condition compared to WT upon dehydration condition (Fig. 7c), indicating that VIL1 functions to limit the induction of *RD29A* under drought conditions. This is similar to the de-repression of *ABI3,* and *ABI4* observed in response to the ABA treatment in *vil1* mutants. Therefore, we determined whether *RD29A* chromatin is also a direct target of VIL1 (Fig. 7e,f). Indeed, VIL1 directly associates with *RD29A* chromatin. However, the dehydration condition does not change the level of VIL1 enrichment at *RD29A* (Fig. 7g). We also determined the enrichment of H3K27me3 at *RD29A*, but the level of H3K27me3 does not change by the dehydrating treatment (Fig. 7h). However, the level of H3K27me3 at *RD29A* is reduced in *vil1* mutants (Fig. 7h), indicating that the reduced level of H3K27me3 contributes to the increased induction of *RD29A* upon dehydration in *vil1* mutants.

Discussion

Previous studies showed that PHD-finger protein VIL1 is a facultative subunit of VRN2-PRC2 and is required for the repression of *FLC* in response to winter cold (Sung *et al.*, 2006; Greb *et al.*, 2007; De Lucia *et al.*, 2008). Similar facultative subunits of PRC2 are present in other eukaryotes, such as Pcl-PRC2 of *Drosophila* and PHF1-PRC2 of animals (Hennig & Derkacheva, 2009). *In vitro* studies have shown that the mammalian PHD finger protein, PHF1, promotes the ability of EZH2 to catalyze H3K27me3 of its target chromatin (Sarma *et al.*, 2008). Similarly, VIL1-PRC2 directly associates with *FLC* and is necessary for the H3K27me3 enrichment at the *FLC* chromatin by vernalization (Sung *et al.*, 2006; Greb *et al.*, 2007). Two E(z) homologs, CLF and SWN, are functionally redundant in PRC2 complexes in the sporophyte (Chanvivattana *et al.*, 2004) and are necessary for proper development. The *clf swn* double mutant is pleiotropic, and its development is arrested at early seedling stages, indicating the involvement of PRC2 in a wide range of developmental processes (Chanvivattana *et al.*, 2004; Hennig & Derkacheva, 2009; Farrona *et al.*, 2011; Mozgova & Hennig, 2015; Shu *et al.*, 2019). On the other hand, mutations in facultative

components of PRC2, such as VIL1, compromise only subsets of PRC2-regulated loci, as shown in this study.

It has been reported that the conditional *fie* mutants exhibit enhanced dormancy and germination defects, indicating the possible roles of PRC2 in the ABA response (Bouyer *et al.*, 2011). The conditional *fie* mutants also caused severe growth defects, similar to *clf swn* double mutants (Bouyer *et al.*, 2011). Therefore, it is difficult to address whether the defects shown in the early seedling stage reflect the direct involvement of *FIE* or the secondary effect due to the pleiotropic phenotypes observed in *fie* mutants. A study using the weak double mutant *clf-50 swn-1*, in which *swn-1* is a hypomorphic allele, accelerated leaf senescence by the ABA treatment in *Arabidopsis*, a hyposensitive response to the ABA treatment (Liu *et al.*, 2019). The CLF/SWN-mediated H3K27me3 limits the ABA-induced senescence-associated genes and thus delays the leaf senescence (Liu *et al.*, 2019). It has also been reported that the *clf* mutant is more sensitive to dehydration treatment, implying the hyposensitive response to the ABA treatment in *clf* mutants (Liu *et al.*, 2014). Therefore, the role of core Polycomb in the ABA responses is somewhat complicated in part due to developmental defects observed in Polycomb mutants.

However, *vil1* mutants do not exhibit severe developmental defects other than hypersensitivity to the ABA treatment during early seedling development. The level of endogenous ABA rapidly declines after germination (Weitbrecht *et al.*, 2011), and the ABA-responsive genes, such as *ABI3*, *ABI4,* and *ABI5*, are quickly repressed after germination. We show that VIL1 directly associates with two ABA-signaling upstream transcription factor loci, *ABI3* and *ABI4*, to repress them effectively by facilitating H3K27me3 during early seedling formation (Fig. 2). In addition, the ABA-induced expression of *ABI3* and *ABI4* also include the rapid reduction of the enrichment of VIL1 and H3K27me3 (Fig. 2 and Fig. 3), indicating the dynamic roles of VIL1-mediated H3K27me3 in the ABA-mediated transcriptional regulation. However, there is no rapid reduction in the enrichment of core PRC2 components in response to ABA, suggesting that Polycomb utilizes a facultative component to fine-tune its chromatin remodeling activity. Therefore, our work demonstrates that a facultative component of PRC2, such as VIL1, provides a flexible regulatory module to control its chromatin-modifying activity in response to developmental and hormonal signals.

Upon the deprivation of ABA, inactive SnRK2 would likely diminish the pool of activating transcription factors to initiate transcriptional cascades. In parallel, our study shows that VIL1-PRC2 functions to ensure the proper repression of ABA-responsive genes during early seedling establishment by directly mediating the deposition of a repressive histone modification, H3K27me3, at *ABI3* and *ABI4* (Fig. S10). Although the reduction in H3K27me3 levels at *ABI3* and *ABI4* correlates with the eviction of VIL1 (Fig. 2c,d), the degree of H3K27me3 reduction by ABA treatment is more severe than in *vil1* mutants (Fig. 3a,b). This suggests that there are other factors contributing to the reduction of H3K27me3 by ABA. It remains to be determined whether ABA-signaling components directly dictate recruitment and/or eviction of VIL1 and/or other Polycomb proteins.

Many stress-induced genes have been targeted for the potential candidate genes to improve tolerance to stress conditions in plants by genetic engineering. Over- and/or under-expression of such genes have shown to effectively improve resistance to certain stress conditions (Zhang *et al.*, 2020). However, simple constitutive expression of stress-induced genes often results in developmental or growth defects (Martignago *et al.*, 2019). Therefore, inducible promoter-driven strategies have been most successful (Kasuga *et al.*, 1999). It should be noted that *vil1* mutants do not show extreme ectopic expression of stress-responsive genes in the absence of stimuli (Table S2). Instead, VIL1-mediated H3K27me3 appears to limit the degree of induction of *RD29A* under drought conditions (Fig. 7e). Therefore, a mild but significant increase in the level of transcriptional induction of *RD29A* results in unexpected drought tolerance without compromising the growth of plants in *vil1* mutants.

Supplementary Material

Refer to Web version on PubMed Central for supplementary material.

Acknowledgment

We thank Dr. Yuhai Cui (Western University, Canada) for p*CLF*::*CLF-GFP*/*clf29* (*gCLF-GFP*) and p*SWN*::*SWN-GFP*/*swn-4* (*gSWN-GFP*) seeds. This work was supported by NIH R01GM100108, NSF IOS 1656764 to S. S., and NIH R01GM115879 to H. Q.

Data Availability

The data discussed in this publication have been deposited in NCBI Gene Expression Omnibus and are accessible through GEO series accession no. GSE180587.

Reference

Baroux C, Gagliardini V, Page DR, Grossniklaus U. 2006. Dynamic regulatory interactions of Polycomb group genes: MEDEA autoregulation is required for imprinted gene expression in *Arabidopsis*. Genes Dev 20(9): 1081–1086. [PubMed: 16651654]

Bossi F, Cordoba E, Dupre P, Mendoza MS, Roman CS, Leon P. 2009. The *Arabidopsis* ABA-INSENSITIVE (ABI) 4 factor acts as a central transcription activator of the expression of its own gene, and for the induction of ABI5 and SBE2.2 genes during sugar signaling. Plant J 59(3): 359–374. [PubMed: 19392689]

Bouyer D, Roudier F, Heese M, Andersen ED, Gey D, Nowack MK, Goodrich J, Renou JP, Grini PE, Colot V, et al. 2011. Polycomb repressive complex 2 controls the embryo-to-seedling phase transition. PLoS Genet 7(3): e1002014. [PubMed: 21423668]

Bulgakov VP, Wu HC, Jinn TL. 2019. Coordination of ABA and Chaperone Signaling in Plant Stress Responses. Trends Plant Sci 24(7): 636–651. [PubMed: 31085125]

Chandrasekaran U, Luo X, Zhou W, Shu K. 2020. Multifaceted Signaling Networks Mediated by Abscisic Acid Insensitive 4. Plant Commun 1(3): 100040. [PubMed: 33367237]

Chanvivattana Y, Bishopp A, Schubert D, Stock C, Moon YH, Sung ZR, Goodrich J. 2004. Interaction of Polycomb-group proteins controlling flowering in *Arabidopsis*. Development 131(21): 5263–5276. [PubMed: 15456723]

Chen C, Chen H, Zhang Y, Thomas HR, Frank MH, He Y, Xia R. 2020. TBtools: An Integrative Toolkit Developed for Interactive Analyses of Big Biological Data. Mol Plant 13(8): 1194–1202. [PubMed: 32585190]

Chen K, Li GJ, Bressan RA, Song CP, Zhu JK, Zhao Y. 2020. Abscisic acid dynamics, signaling, and functions in plants. J Integr Plant Biol 62(1): 25–54. [PubMed: 31850654]

Ciferri C, Lander GC, Maiolica A, Herzog F, Aebersold R, Nogales E. 2012. Molecular architecture of human polycomb repressive complex 2. Elife 1: e00005. [PubMed: 23110252]

Clough SJ, Bent AF. 1998. Floral dip: a simplified method for Agrobacterium-mediated transformation of *Arabidopsis thaliana*. Plant J 16(6): 735–743. [PubMed: 10069079]

Cutler SR, Rodriguez PL, Finkelstein RR, Abrams SR. 2010. Abscisic acid: emergence of a core signaling network. Annu Rev Plant Biol 61: 651–679. [PubMed: 20192755]

De Lucia F, Crevillen P, Jones AM, Greb T, Dean C. 2008. A PHD-polycomb repressive complex 2 triggers the epigenetic silencing of *FLC* during vernalization. Proc Natl Acad Sci U S A 105(44): 16831–16836. [PubMed: 18854416]

Derkacheva M, Steinbach Y, Wildhaber T, Mozgova I, Mahrez W, Nanni P, Bischof S, Gruissem W, Hennig L. 2013. Arabidopsis MSI1 connects LHP1 to PRC2 complexes. EMBO J 32(14): 2073–2085. [PubMed: 23778966]

Farrona S, Thorpe FL, Engelhorn J, Adrian J, Dong X, Sarid-Krebs L, Goodrich J, Turck F. 2011. Tissue-specific expression of *FLOWERING LOCUS T* in *Arabidopsis* is maintained independently of polycomb group protein repression. Plant Cell 23(9): 3204–3214. [PubMed: 21917549]

Feng CZ, Chen Y, Wang C, Kong YH, Wu WH, Chen YF. 2014. *Arabidopsis* RAV1 transcription factor, phosphorylated by SnRK2 kinases, regulates the expression of *ABI3*, *ABI4*, and *ABI5* during seed germination and early seedling development. Plant J 80(4): 654–668. [PubMed: 25231920]

Finkelstein RR, Gampala SS, Rock CD. 2002. Abscisic acid signaling in seeds and seedlings. Plant Cell 14 Suppl: S15–45. [PubMed: 12045268]

Finkelstein RR, Lynch TJ. 2000. The Arabidopsis abscisic acid response gene *ABI5* encodes a basic leucine zipper transcription factor. Plant Cell 12(4): 599–609. [PubMed: 10760247]

Finkelstein RR, Wang ML, Lynch TJ, Rao S, Goodman HM. 1998. The Arabidopsis abscisic acid response locus *ABI4* encodes an APETALA 2 domain protein. Plant Cell 10(6): 1043–1054. [PubMed: 9634591]

Fujii H, Chinnusamy V, Rodrigues A, Rubio S, Antoni R, Park SY, Cutler SR, Sheen J, Rodriguez PL, Zhu JK. 2009. In vitro reconstitution of an abscisic acid signalling pathway. Nature 462(7273): 660–664. [PubMed: 19924127]

Gendall AR, Levy YY, Wilson A, Dean C. 2001. The VERNALIZATION 2 gene mediates the epigenetic regulation of vernalization in *Arabidopsis*. Cell 107(4): 525–535. [PubMed: 11719192]

Giraudat J, Hauge BM, Valon C, Smalle J, Parcy F, Goodman HM. 1992. Isolation of the *Arabidopsis ABI3* gene by positional cloning. Plant Cell 4(10): 1251–1261. [PubMed: 1359917]

Greb T, Mylne JS, Crevillen P, Geraldo N, An H, Gendall AR, Dean C. 2007. The PHD finger protein VRN5 functions in the epigenetic silencing of *Arabidopsis FLC*. Curr Biol 17(1): 73–78. [PubMed: 17174094]

Gubler F, Millar AA, Jacobsen JV. 2005. Dormancy release, ABA and pre-harvest sprouting. Curr Opin Plant Biol 8(2): 183–187. [PubMed: 15752999]

Hennig L, Derkacheva M. 2009. Diversity of Polycomb group complexes in plants: same rules, different players? Trends Genet 25(9): 414–423. [PubMed: 19716619]

Jia H, Suzuki M, McCarty DR. 2014. Regulation of the seed to seedling developmental phase transition by the LAFL and VAL transcription factor networks. Wiley Interdiscip Rev Dev Biol 3(1): 135–145. [PubMed: 24902838]

Kasuga M, Liu Q, Miura S, Yamaguchi-Shinozaki K, Shinozaki K. 1999. Improving plant drought, salt, and freezing tolerance by gene transfer of a single stress-inducible transcription factor. Nat Biotechnol 17(3): 287–291. [PubMed: 10096298]

Kim DH, Sung S. 2013. Coordination of the Vernalization Response through a *VIN3* and *FLC* Gene Family Regulatory Network in Arabidopsis. Plant Cell 25(2): 454–469. [PubMed: 23417034]

Kim J, Bordiya Y, Kathare PK, Zhao B, Zong W, Huq E, Sung S. 2021. Phytochrome B triggers light-dependent chromatin remodelling through the PRC2-associated PHD finger protein VIL1. Nat Plants 7(9):1213–1219. [PubMed: 34354260]

Kim SY, Lee J, Eshed-Williams L, Zilberman D, Sung ZR. 2012. EMF1 and PRC2 cooperate to repress key regulators of Arabidopsis development. PLoS Genet 8(3): e1002512. [PubMed: 22457632]

Lee HG, Seo PJ. 2019. MYB96 recruits the HDA15 protein to suppress negative regulators of ABA signaling in Arabidopsis. Nat Commun 10(1): 1713. [PubMed: 30979883]

Liu C, Cheng J, Zhuang Y, Ye L, Li Z, Wang Y, Qi M, Xu L, Zhang Y. 2019. Polycomb repressive complex 2 attenuates ABA-induced senescence in *Arabidopsis*. Plant J 97(2): 368–377. [PubMed: 30307069]

Liu H, Ding Y, Zhou Y, Jin W, Xie K, Chen LL. 2017. CRISPR-P 2.0: An Improved CRISPR-Cas9 Tool for Genome Editing in Plants. Mol Plant 10(3): 530–532. [PubMed: 28089950]

Liu N, Fromm M, Avramova Z. 2014. H3K27me3 and H3K4me3 chromatin environment at super-induced dehydration stress memory genes of *Arabidopsis thaliana*. Mol Plant 7(3): 502–513. [PubMed: 24482435]

Lopez-Molina L, Mongrand S, Chua NH. 2001. A postgermination developmental arrest checkpoint is mediated by abscisic acid and requires the ABI5 transcription factor in Arabidopsis. Proc Natl Acad Sci U S A 98(8): 4782–4787. [PubMed: 11287670]

Lopez-Molina L, Mongrand S, McLachlin DT, Chait BT, Chua NH. 2002. ABI5 acts downstream of ABI3 to execute an ABA-dependent growth arrest during germination. Plant J 32(3): 317–328. [PubMed: 12410810]

Ma Y, Szostkiewicz I, Korte A, Moes D, Yang Y, Christmann A, Grill E. 2009. Regulators of PP2C phosphatase activity function as abscisic acid sensors. Science 324(5930): 1064–1068. [PubMed: 19407143]

Martignago D, Rico-Medina A, Blasco-Escamez D, Fontanet-Manzaneque JB, Cano-Delgado AI. 2019. Drought Resistance by Engineering Plant Tissue-Specific Responses. Front Plant Sci 10: 1676. [PubMed: 32038670]

Mozgova I, Hennig L. 2015. The Polycomb Group Protein Regulatory Network. Annual Review of Plant Biology, Vol 66 66: 269–296.

Nakashima K, Fujita Y, Katsura K, Maruyama K, Narusaka Y, Seki M, Shinozaki K, Yamaguchi-Shinozaki K. 2006. Transcriptional regulation of ABI3- and ABA-responsive genes including *RD29B* and *RD29A* in seeds, germinating embryos, and seedlings of Arabidopsis. Plant Mol Biol 60(1): 51–68. [PubMed: 16463099]

Nambara E, Keith K, McCourt P, Naito S. 1994. Isolation of an internal deletion mutant of the Arabidopsis thaliana ABI3 gene. Plant Cell Physiol 35(3): 509–513. [PubMed: 8055176]

Parcy F, Valon C, Kohara A, Misera S, Giraudat J. 1997. The *ABSCISIC ACID-INSENSITIVE3*, *FUSCA3*, and *LEAFY COTYLEDON1* loci act in concert to control multiple aspects of Arabidopsis seed development. Plant Cell 9(8): 1265–1277. [PubMed: 9286105]

Park SY, Fung P, Nishimura N, Jensen DR, Fujii H, Zhao Y, Lumba S, Santiago J, Rodrigues A, Chow TF, et al. 2009. Abscisic acid inhibits type 2C protein phosphatases via the PYR/PYL family of START proteins. Science 324(5930): 1068–1071. [PubMed: 19407142]

Peirats-Llobet M, Han SK, Gonzalez-Guzman M, Jeong CW, Rodriguez L, Belda-Palazon B, Wagner D, Rodriguez PL. 2016. A Direct Link between Abscisic Acid Sensing and the Chromatin-Remodeling ATPase BRAHMA via Core ABA Signaling Pathway Components. Mol Plant 9(1): 136–147. [PubMed: 26499068]

Perruc E, Kinoshita N, Lopez-Molina L. 2007. The role of chromatin-remodeling factor PKL in balancing osmotic stress responses during Arabidopsis seed germination. Plant J 52(5): 927–936. [PubMed: 17892443]

Sarma K, Margueron R, Ivanov A, Pirrotta V, Reinberg D. 2008. Ezh2 requires PHF1 to efficiently catalyze H3 lysine 27 trimethylation in vivo. Mol Cell Biol 28(8): 2718–2731. [PubMed: 18285464]

Shu J, Chen C, Thapa RK, Bian S, Nguyen V, Yu K, Yuan ZC, Liu J, Kohalmi SE, Li C, et al. 2019. Genome-wide occupancy of histone H3K27 methyltransferases CURLY LEAF and SWINGER in Arabidopsis seedlings. Plant Direct 3(1): e00100. [PubMed: 31245749]

Sung S, Schmitz RJ, Amasino RM. 2006. A PHD finger protein involved in both the vernalization and photoperiod pathways in Arabidopsis. Genes Dev 20(23): 3244–3248. [PubMed: 17114575]

Tian T, Liu Y, Yan H, You Q, Yi X, Du Z, Xu W, Su Z. 2017. agriGO v2.0: a GO analysis toolkit for the agricultural community, 2017 update. Nucleic Acids Res 45(W1): W122–W129. [PubMed: 28472432]

To A, Valon C, Savino G, Guilleminot J, Devic M, Giraudat J, Parcy F. 2006. A network of local and redundant gene regulation governs Arabidopsis seed maturation. Plant Cell 18(7): 1642–1651. [PubMed: 16731585]

Wang H, Liu C, Cheng J, Liu J, Zhang L, He C, Shen WH, Jin H, Xu L, Zhang Y. 2016. Arabidopsis Flower and Embryo Developmental Genes are Repressed in Seedlings by Different Combinations of Polycomb Group Proteins in Association with Distinct Sets of Cis-regulatory Elements. PLoS Genet 12(1): e1005771. [PubMed: 26760036]

Wang ZP, Xing HL, Dong L, Zhang HY, Han CY, Wang XC, Chen QJ. 2015. Egg cell-specific promoter-controlled CRISPR/Cas9 efficiently generates homozygous mutants for multiple target genes in *Arabidopsis* in a single generation. Genome Biol 16: 144. [PubMed: 26193878]

Weitbrecht K, Muller K, Leubner-Metzger G. 2011. First off the mark: early seed germination. J Exp Bot 62(10): 3289–3309. [PubMed: 21430292]

Xing HL, Dong L, Wang ZP, Zhang HY, Han CY, Liu B, Wang XC, Chen QJ. 2014. A CRISPR/Cas9 toolkit for multiplex genome editing in plants. BMC Plant Biol 14: 327. [PubMed: 25432517]

Yu JR, Lee CH, Oksuz O, Stafford JM, Reinberg D. 2019. PRC2 is high maintenance. Genes & Development 33(15–16): 903–935. [PubMed: 31123062]

Zhang H, Zhao Y, Zhu JK. 2020. Thriving under Stress: How Plants Balance Growth and the Stress Response. Dev Cell 55(5): 529–543. [PubMed: 33290694]

Zong W, Zhao B, Xi Y, Bordiya Y, Mun H, Cerda NA, Kim DH, Sung S. 2021. DEK domain-containing proteins control flowering time in *Arabidopsis*. New Phytol. 231 (1), 182–192. [PubMed: 33774831]

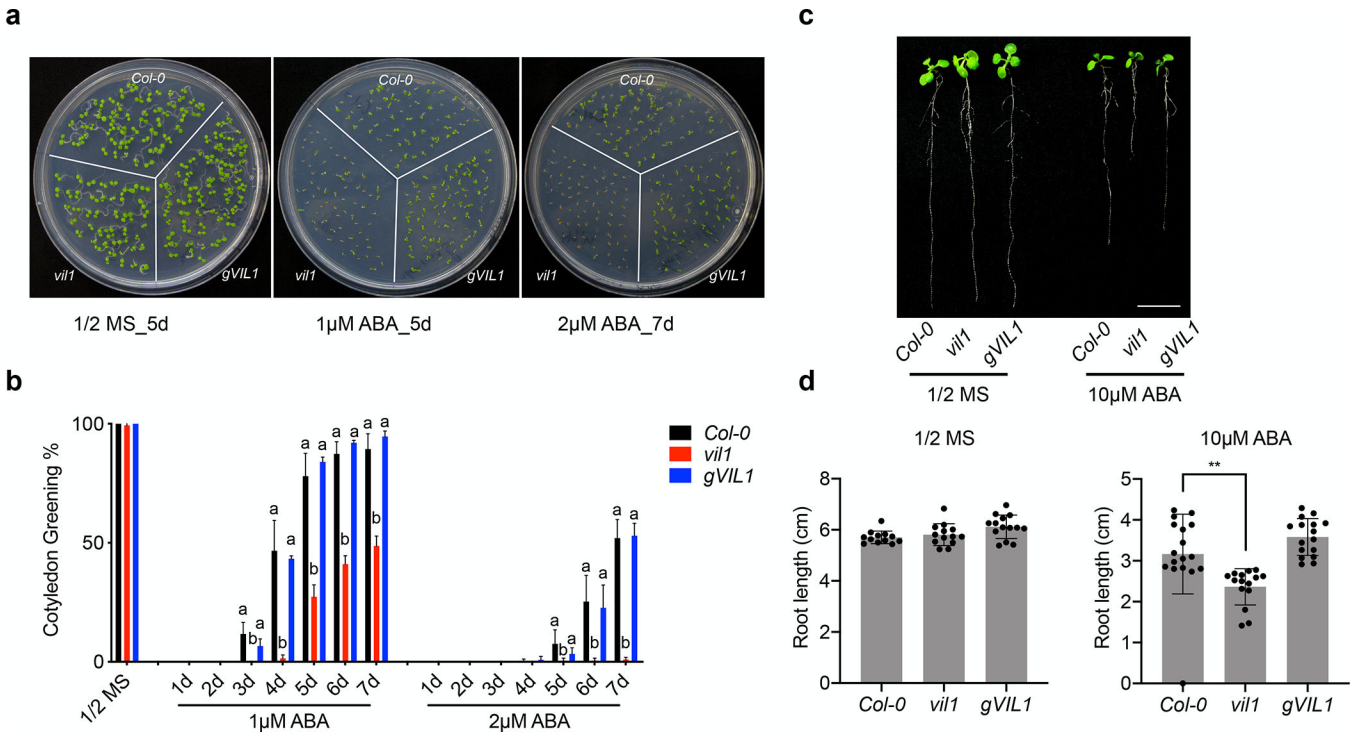

Fig. 1.

vil1 mutant shows increased ABA sensitivity in *Arabidopsis*. (a) Germination phenotypes of WT, *vil1* mutants, and complement lines (*gVIL1-cMYC, gVIL1*) in the presence of 1 μM or 2 μM ABA. (b) The percentage of germinated embryos that developed green cotyledons in the presence of 1 μM or 2 μM ABA in the Col-0, *vil1,* and *gVIL1*. Values are mean ± s. d. (n = 3; each set includes more than 60 seeds). One-way ANOVA Tukey's multiple comparison test was conducted; letters indicate $P < 0.05$ of distinct groups. (c) Root phenotype of Col-0, *vil1,* and *gVIL1* plants grown under 1/2 MS medium or 1/2 MS medium containing 10 μM ABA for 7 days. White scale bar = 1 cm. (d) Primary root length of seedlings treated as described in (c). The black dots indicate individual measurement. Data are presented as the means ± s. d. (n = 15). **$P < 0.01$, significant difference using Student's t-test.

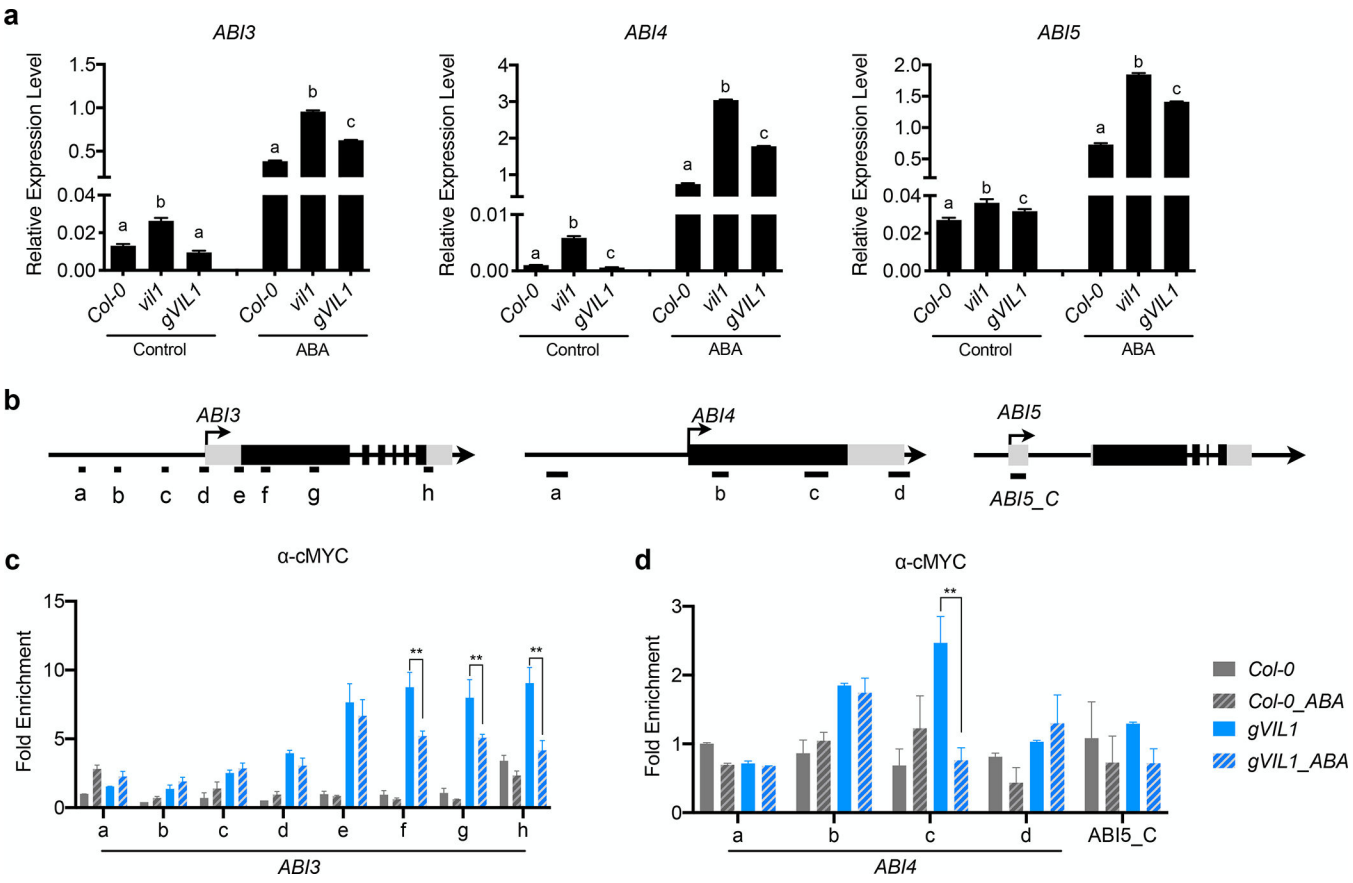

Fig. 2.

VIL1 directly and negatively regulates the expression of *ABI3* and *ABI4* in *Arabidopsis*. (a) Relative expression of *ABI3*, *ABI4,* and *ABI5* in Col-0, *vil1,* and *gVIL1* seedlings germinated with or without ABA. Stratified Col-0, *vil1,* and *gVIL1* seeds were germinated with (ABA) or without (Control) 0.5 μM ABA for 3 days. Transcript levels were normalized to the level of *PP2A*. Error bars: ± s. d. ($n = 3$). One-way ANOVA Tukey's multiple comparison test was conducted; letters indicate $P < 0.05$ of distinct groups. (b) Schematic diagram showing the genome regions of *ABI3, ABI4*, and *ABI5*. Exons are represented by black boxes, while black lines between exons represent introns. Black arrows with vertical lines indicate transcription start sites and direction of arrows indicate the orientation of transcription. DNA fragments amplified in ChIP assays are labeled beneath the genomic regions. (c and d) Analysis of the VIL1 binding to *ABI3, ABI4,* and *ABI5* genomic regions with or without 0.5 μM ABA for 3 days. Enriched values were normalized to the level of input DNA, and the relative fold enrichment over Col-0 is presented. Error bars: ± s. d. ($n = 3$). (c,d) **$P < 0.01$. Significant difference using Student's *t*-test.

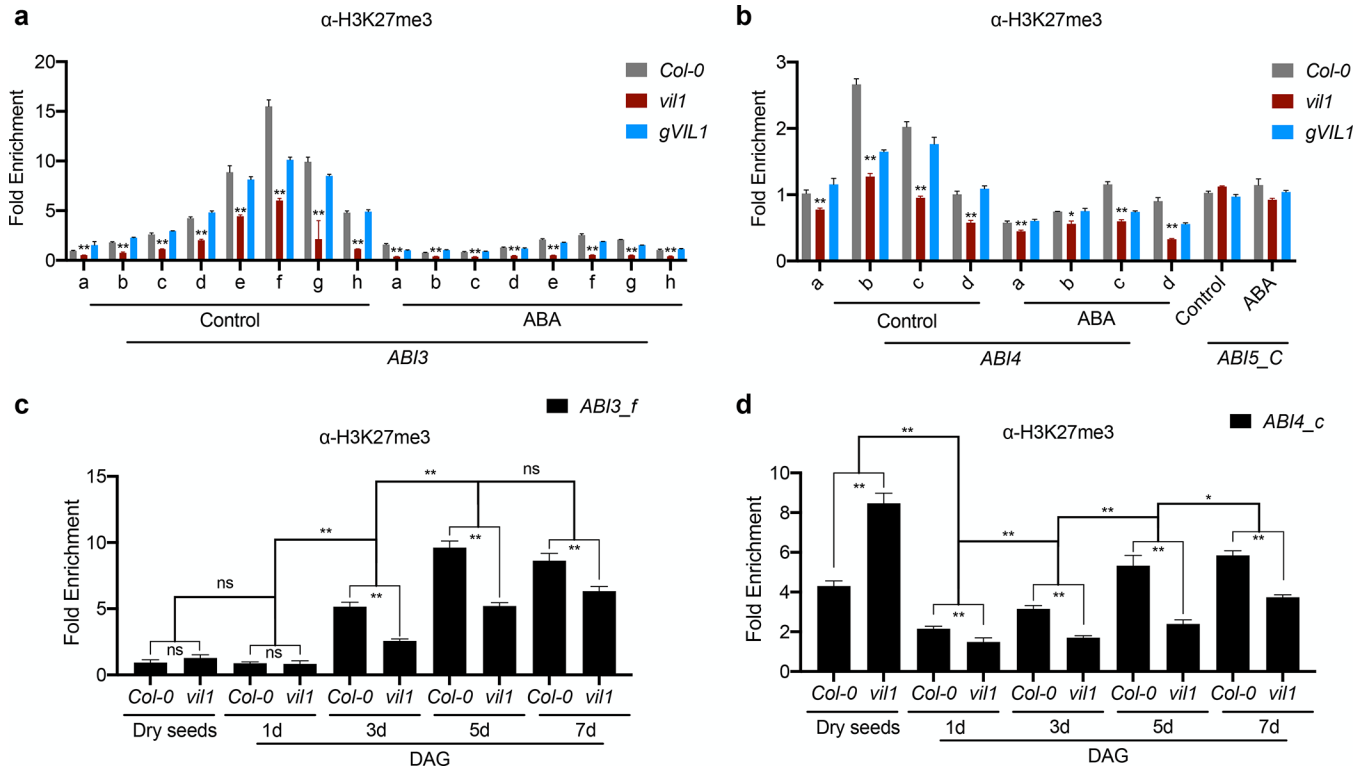

Fig. 3.

VIL1 is necessary for the H3K27me3 enrichment at *ABI3* and *ABI4* loci in *Arabidopsis*. (a and b). ChIP-qPCR analysis of H3K27me3 at *ABI3*, *ABI4,* and *ABI5* loci in the *Col-0*, *vil1-1,* and *gVIL1* seedlings germinated with (ABA) or without (Control) 0.5 μM ABA for 3 days. Each examined region was normalized to Input and error bars: ± s. d. ($n = 3$). *P < 0.05, **P <0.01, Significant difference using Student's *t*-test. (c and d) ChIP-qPCR analysis of H3K27me3 levels at *ABI3* and *ABI4* at different germination stages of the Col-0 and *vil1-1.* For dry seeds of Col-0 and *vil1*, seeds were sterilized and imbibed in water for 30 mins and then harvested for ChIP analysis. For germinated seeds, Col-0 and *vil1* seeds were first sterilized and stratified at 4°C for 3 days and then germinated at 22°C with 16h light /8h dark condition. Each examined region (depicted in Fig. 2b) was normalized to *TA3* and error bars: ± s. d. ($n = 3$). *P < 0.05, **P < 0.01, ns no significant differences between distinct groups. Significant difference using Student's *t*-test.

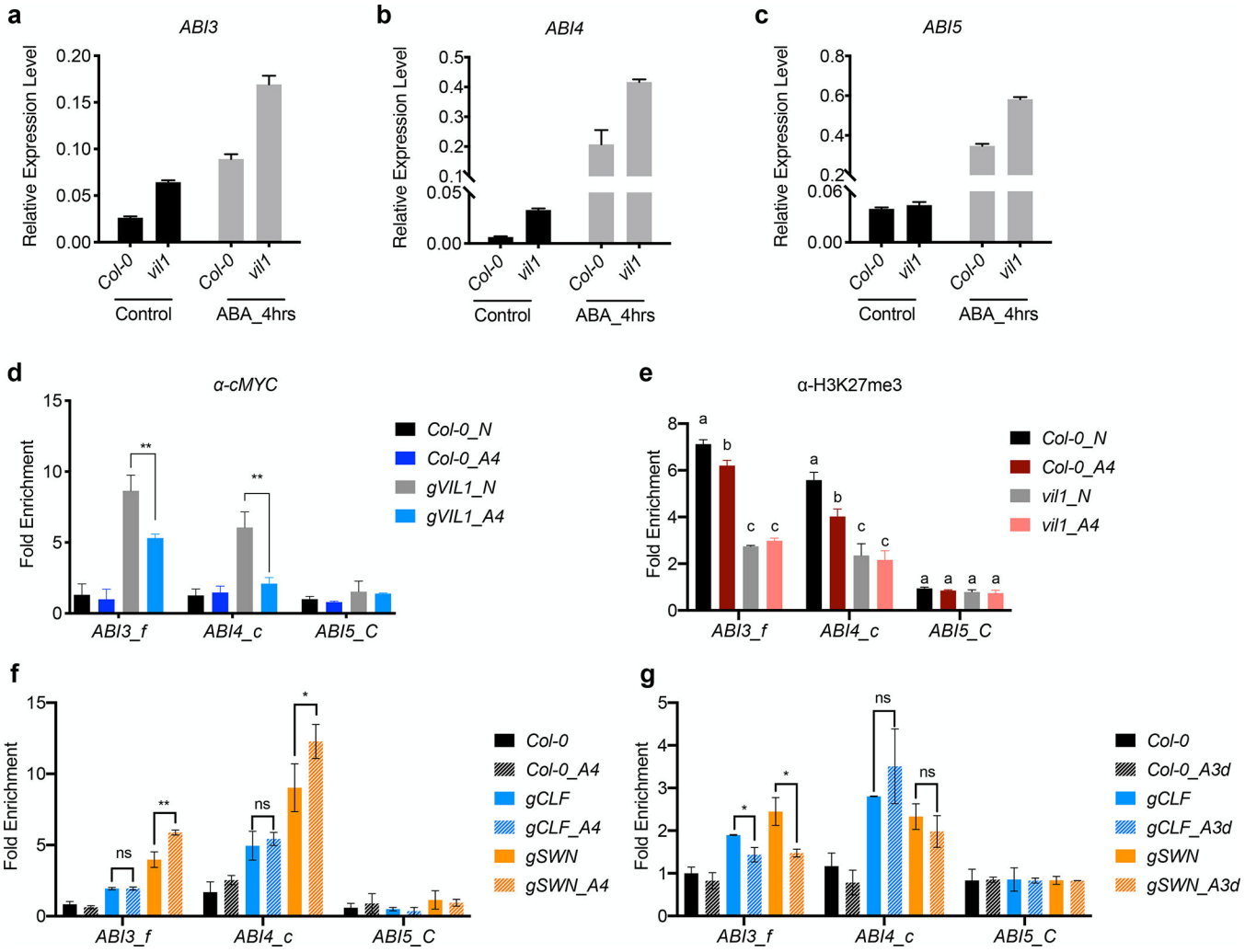

Fig. 4.

ABA inhibits the H3K27me3 at *ABI3* and *ABI4* loci in *Arabidopsis*. (a-c) Relative expression of *ABI3* (a), *ABI4* (b) and *ABI5* (c) in Col-0 and *vil1* seedlings treated with or without ABA. 3-day-old Col-0 and *vil1* seedlings were treated with (ABA_4hrs) or without (Control) 50 μM ABA for 4 hours. Transcript levels were normalized to *PP2A* and error bars: ±s. d. (n=3). (d) Analysis of VIL1 binding to *ABI3* and *ABI4* genomic regions in seedlings treated with or without ABA by ChIP-qPCR. 3-day-old seedlings of Col-0 and *gVIL1* were treated with or without 50 μM ABA for 4 hours. Enriched values were normalized with the level of input DNA and relative fold enrichment over Col-0 are presented. Error bars: ± s. d. (n = 3). *ABI5* was used as a negative control. **P < 0.01, significant difference using Student's t-test. (e) ChIP-qPCR analysis of H3K27me3 levels at *ABI3* and *ABI4* in WT and *vil1* seedlings treated with or without ABA. Each examined region was normalized to the retrotransposon *TA3* and error bars: ± s. d. (n = 3). *ABI5* was used as a negative control. One-way ANOVA Tukey's multiple comparison test was conducted; letters indicate P < 0.05 of distinct groups. (f and g) Analysis of CLF and SWN binding to *ABI3* and *ABI4* under short-term (f) and long-term (g) ABA treatment by ChIP-qPCR. For short-term ABA treatment (A4), 3-day-old seedlings of *gCLF_GFP,*

gSWN_GFP and control (Col-0) treated with or without 50 μM ABA for 4 hours were used in ChIP assay. For long-term ABA treatment (A3d), Col-0, *gCLF_GFP* and *gSWN_GFP* seedlings that germinated with or without 0.5 μM ABA for 3 days were used in ChIP assay. Fragments immunoprecipitated by anti-GFP were quantified by qPCR and normalized to *TA3*. Relative levels in gCLF_GFP and gSWN_GFP over control are presented and error bars: ± s. d. (n = 3). *ABI5* was used as a negative control. *P < 0.05, **P < 0.01, ns no significant differences between distinct groups, significant difference using Student's *t*-test.

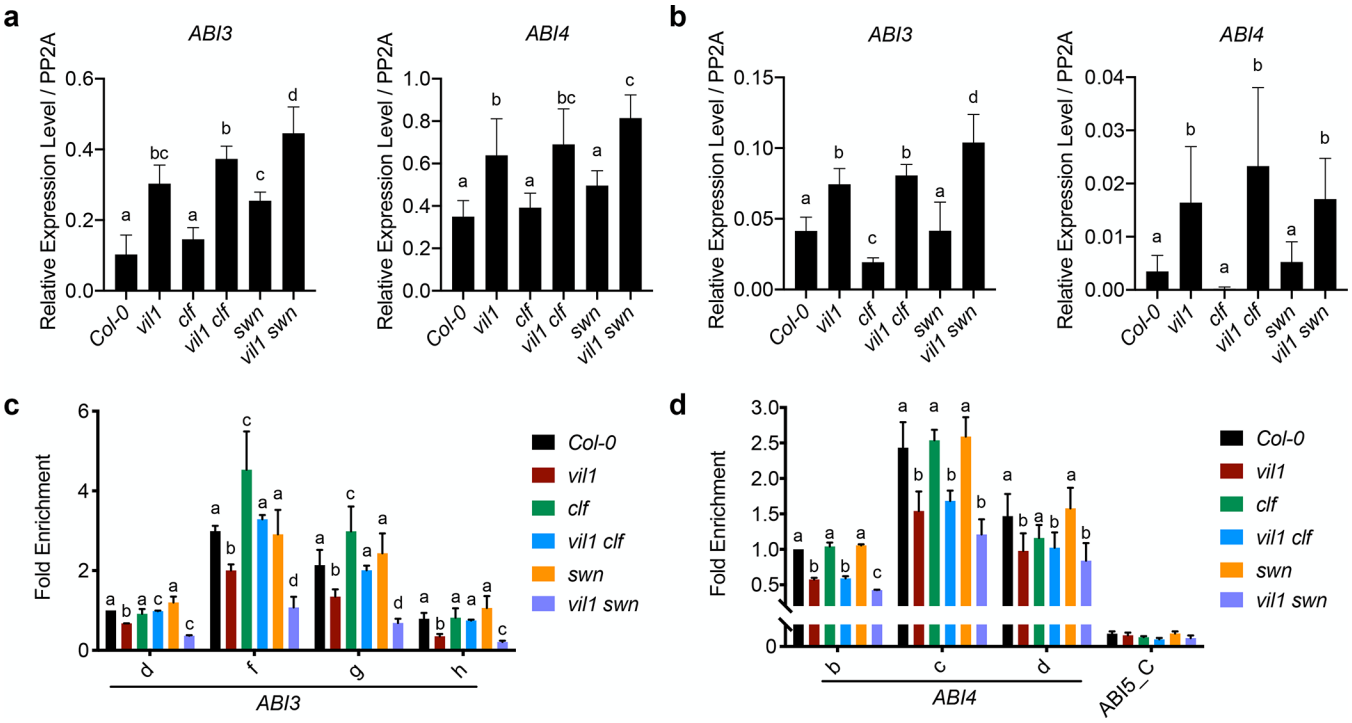

Fig. 5.

VIL1 promotes the function of both CLF and SWN of PRC2 in *Arabidopsis*. (a and b) RT-qPCR analysis of *ABI3* and *ABI4* expression in 1-day (a) and 3-day (b) germinated seeds of the indicated genotypes. Transcript levels were normalized to *PP2A* and error bars: ± s. d. ($n = 3$). (c and d) ChIP-qPCR analysis of the H3K27me3 levels at *ABI3* (c) and *ABI4* (d) loci in indicated genotypes. 3-day-old seedlings of Col-0, *vil1*, *clf*, *vil1 clf*, *swn,* and *vil1 swn* are used in ChIP assay. Each examined region was normalized to *TA3*. Error bars: ± s. d. ($n = 3$). One-way ANOVA Tukey's multiple comparison test was conducted; letters indicate $P < 0.05$ of distinct groups.

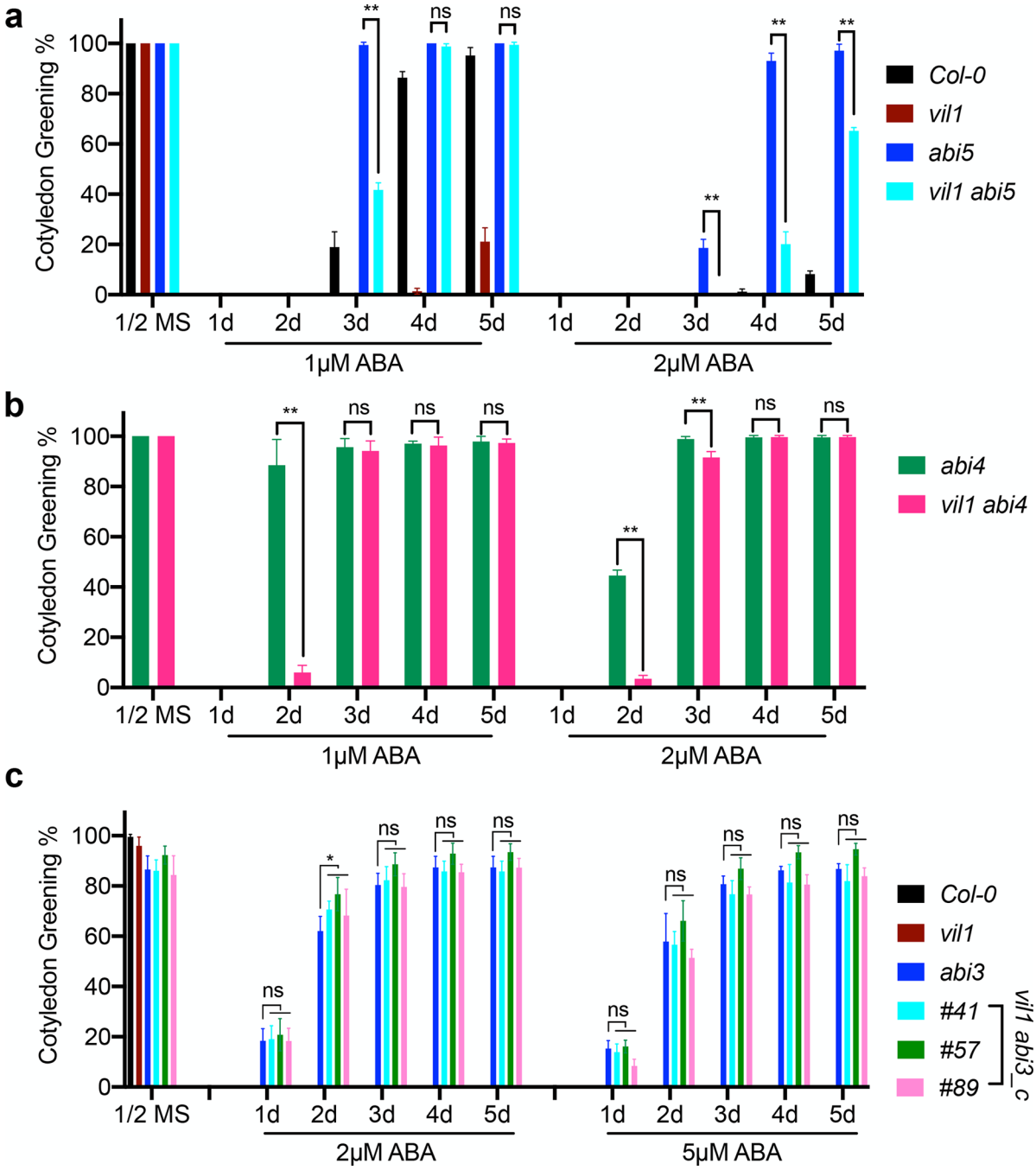

Fig. 6.

VIL1 regulates the ABA response through *ABI3* and *ABI4* in *Arabidopsis.* (a and b) ABA response of indicated genotypes. Green cotyledon percentage of seeds grown on 1/2 MS medium for 3 days or 1/2 MS medium containing 1 μM ABA or 2 μM ABA for indicated days were presented. Values are mean ± s. d. (n = 3). One-way ANOVA Tukey's multiple comparison test was conducted; asterisks indicate P < 0.01 of distinct groups, ns indicates no significant differences of distinct groups. (c) ABA response of *WT*, *vil1*, *abi3* and *vil1 abi3_c* double mutants. Green cotyledon percentage of seeds grown on 1/2 MS medium for

3 days or 1/2 MS medium containing 2 μM ABA or 5 μM ABA for indicated days were presented. Error bars: ± s. d. (n = 3). One-way ANOVA Tukey's multiple comparison test was conducted; asterisks indicate $P < 0.05$ of distinct groups, ns indicate no significant differences of distinct groups.

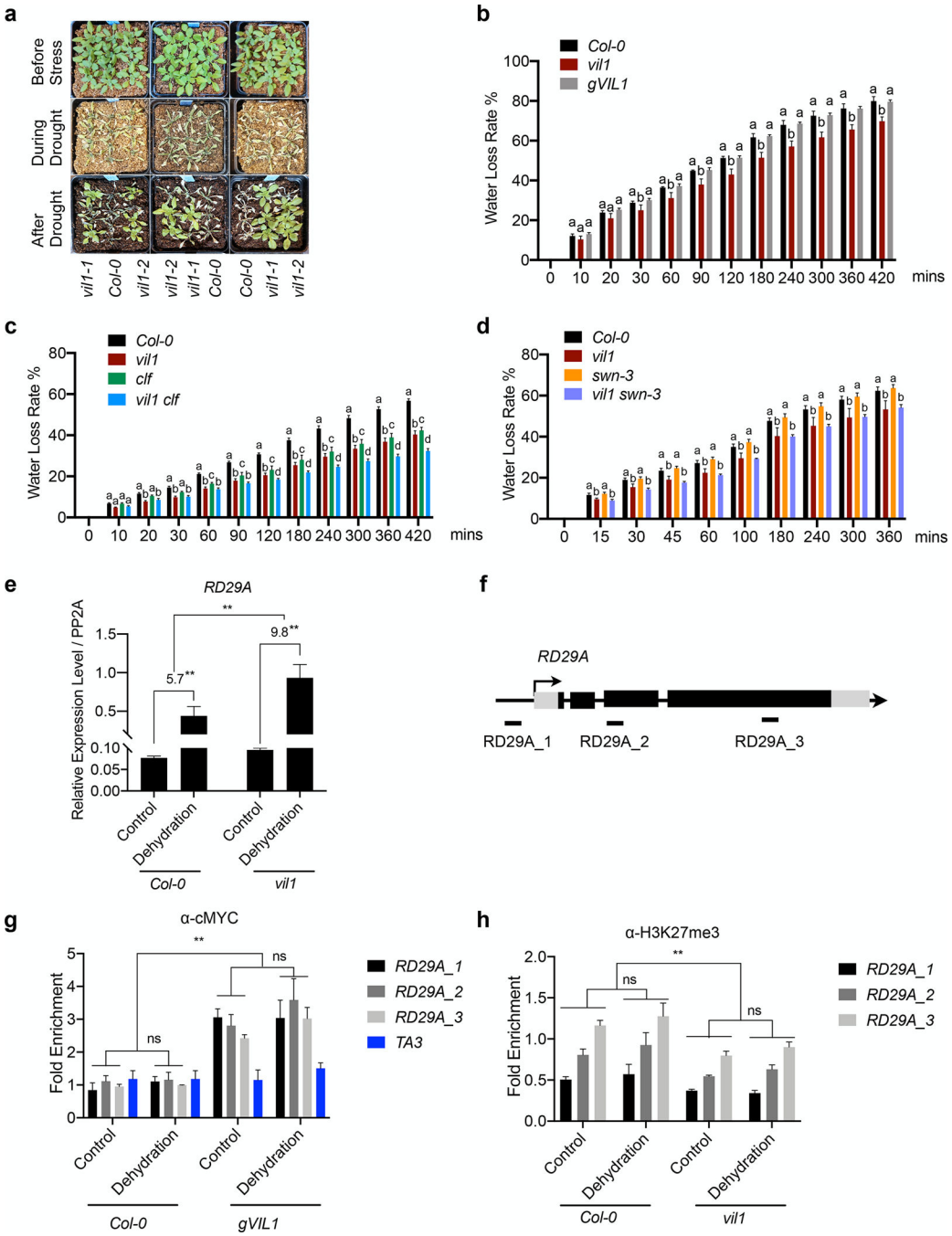

Fig. 7.

Enhanced drought tolerance of *vil1* mutants in *Arabidopsis*. (a) Plant phenotypes for indicated genotypes before and after drought stresses. The phenotype of plants before drought (top), during (middle), and after re-watering (bottom). (b to d) Detached leaf water loss assays. Plants of Col-0, *vil1,* and *gVIL1* are grown in long days (b). Plants of Col-0, *vil1*, *clf,* and *vil1 clf* are grown in short days (c). Plants of Col-0, *vil1*, *swn-3,* and *vil1 swn-3* are grown in long days (d). Leaves with similar developmental stages were detached and weighted at the indicated time. Water loss represents the proportion of total

weight loss compared with initial weight. Error bars: ±s. d. (n = 3). One-way ANOVA Tukey's multiple comparison test was conducted; letters indicate P < 0.05 of distinct groups. (e) RT-qPCR analysis of *RD29A* expression under dehydration stress in Col-0 and *vil1*. Transcript levels were normalized to *PP2A* and error bars: ±s. d. (n = 3). The numbers (5.7 and 9.8) indicate fold changes between control and dehydration conditions in each genotype. (f) Schematic diagram showing the genome regions of *RD29A*. Exons are represented by black boxes, while black lines between exons represent introns. Black arrow with a vertical line indicates the transcription start site and the direction of arrow indicates the orientation of transcription. DNA fragments amplified in ChIP assays are labeled beneath the genomic regions. (g) Analysis of VIL1 binding to *RD29A* genomic regions with or without dehydration treatment for 1 hour. Enriched values were normalized with the level of input DNA and relative fold enrichment over Col-0 are presented. Error bars: ± s. d. (n = 3). (h) ChIP-qPCR analysis of H3K27me3 levels at *RD29A* in the Col-0 *and vil1-1* seedlings with or without dehydration treatment for 1 hour. Each examined region was normalized to *TA3* and error bars: ± s. d. (n = 3). **P < 0.01 and ns indicate no significant differences between distinct groups. Significant difference using Student's t-test.